Transactions of the 15th International Conference on
Structural Mechanics in Reactor Technology (SMiRT-15)
Seoul, Korea, August 15-20, 1999

A Comparison between Japanese and French A16 Defect Assessment Procedures for Fatigue Crack Growth

Takashi Wakai[1], Christophe Poussard[2] and Bernard Drubay[2]

1) JNC OEC, Structural Safety Engineering Group, Japan
2) CEA Saclay, DRN/DMT/SEMT/LISN, France

ABSTRACT

This paper presents the results of a benchmark on fatigue crack growth evaluation for plates subjected to cyclic bending loads. The simplified fatigue crack growth evaluation methods of JNC in JAPAN and A16 procedures proposed by CEA in France are presented. The methods, based on the reference stress approach, are compared with each other. They are found to differ in estimating crack closure, in the expression used for the reference stress solution and in the formulations used to account for plasticity. The methods are then employed to predict the fatigue crack growth behavior observed experimentally. At R=0.1, the methods provide predictions of crack growth in good agreement with the experimental data. At R=–1.0, significant differences are observed between the predictions. The discrepancies are mainly due to the crack closure effect used to calculate the effective stress intensity factor range.

1. Introduction

Benchmark problems on fatigue crack growth have been exchanged between JNC and CEA. The overall objective of the work is to contribute in developing a good understanding of the simplified crack growth evaluation methods applicable to structural integrity assessment of the fast breeder reactor components.

2. Description of the Benchmark Problems

Three benchmark problems are solved. These consist of plates made of an austenitic stainless steel 316L(N) containing a semi-elliptical surface notch subjected to a cyclic bending moment at a load ratio R=0.1. The shape and dimensions of the specimen are shown in ***Fig.1****. One of the test was performed at room temperature [1] and the two others were performed at 650 °C [2, 3]. The loading conditions, the geometry of the plates and the dimensions of the initial notches are given in* ***Table 1****. The membrane stress σ_m and the bending stress σ_b can be calculated elastically. The material properties are given in* ***Table 2****. The cyclic stress-strain curve at room temperature is given in* ***Table*** *3. At 650°C, the RCC-MR [4] expression is used :*

$$\Delta\varepsilon = 100 \times \frac{2(1+\nu)}{3E}\Delta\sigma + \left(\frac{\Delta\sigma}{K}\right)^{1/m} \qquad (1)$$

where, $\Delta\varepsilon$ is the total strain range in %, $\Delta\sigma$ is the stress range in MPa, E and n are Young's modulus and Poisson's ratio at the corresponding temperature and K and m are constants. For this material, K=718 and m=0.319.

The fatigue crack growth rate is estimated using the Paris law expressed as a function of the effective SIF (Stress Intensity Factor) range ΔK_{eff} :

$$\frac{da}{dN} = C_f \cdot (\Delta K_{eff})^{m_f} \qquad (2)$$

where C_f and m_f are material constants given in ***Table 2.***

3. *JNC Simplified Fatigue Crack Growth Evaluation Method*

Using the Newman and Raju solution[5] for a plate containing a semi-elliptical notch, K is calculated using the influence function method based on the principle of superposition. In the calculation, plasticity is accounted for. The membrane stress σ_m is obtained using the cyclic stress-strain curve and a parameter q_{ep} as shown in ***Fig.2(a)****. For the bending stress, ($\varepsilon_{m\cdot b}$, $\sigma_{m\cdot b}$) and ($\varepsilon_{m\,b}$, $\sigma_{m\,b}$) are determined using the cyclic stress-strain curve of the material and a parameter q_{ep} as illustrated in* ***Fig.2(b)****. The resulting elastoplastic stress distribution through the wall thickness is shown in* ***Fig.2(c)****. Assuming that the thickness of the plate equals to 2, the equivalent bending moment corresponding to such a stress distribution on the notch side and the opposite side is estimated using the following simplified equations :*

$$M_{+b} = \int_0^l \left[f\{\varepsilon_m + (\varepsilon_{m+b} - \varepsilon_m)x\} - \sigma_m \right] x dx$$
$$M_{-b} = \int_{-l}^0 \left[f\{\varepsilon_m + (\varepsilon_m - \varepsilon_{m-b})x\} - \sigma_m \right] x dx \qquad (3)$$

The elastoplastic bending moment M_{ep} can be calculated as follows :

$$M_{ep} = Min.\left[(M_{+b} + M_{-b}), M_e \right] \qquad (4)$$

where M_e is the bending moment derived from an elastic calculation :

$$M_e = \int_{-l}^{l} (S_b x) x dx = \frac{2}{3} S_b \qquad (5)$$

The equivalent elastoplastic bending stress σ_b can be calculated using the following equation :

$$\sigma_b = \frac{6 M_{ep}}{2w \cdot t^2} = \frac{3}{2} M_{ep} \qquad (6)$$

The elastic J-integral range ΔJ_{el} is estimated using a crack closure factor q_w :

$$\Delta J_{el} = \frac{\{q_w \cdot (K_{max} - K_{min})\}^2}{E^*}$$
with
$$q_w = (1 - R)^{n-1} \qquad (7)$$

where K_{max} and K_{min} are the maximum and minimum stress intensity factors in the loading cycle, respectively, and $E^*=E$ for plane stress conditions and $E^*=E / (1-\nu^2)$ for plane strain conditions. Assuming that compressive loads do not contribute to crack growth and crack closure effect is negligible, n is defined by :

for $R \geq 0$	$n = 1$	$q_w = 1$
for $R < 0$	$n = 0$	$q_w = 1 / (1-R)$

The elastoplastic J-integral range ΔJ_{ep} is obtained from ΔJ_{el} using a plastic correction factor f_{ep} :

$$\Delta J_{ep} = f_{ep} \cdot \Delta J_{el} \qquad (8)$$

$$f_{ep} = \frac{\sigma_{ref}^{\ 3}}{2\sigma_y^{\ 2} \cdot E \cdot \varepsilon_{ref}} + \frac{E \cdot \varepsilon_{ref}}{\sigma_{ref}}$$

where σ_{ref} is the reference stress calculated at the maximum load of the cycle and ε_{ref} is the corresponding reference strain. σ_y is the 0.2% proof stress derived from the cyclic stress-strain curve of the material. The reference stress is determined using a net section shape function F_{net} :

$$\sigma_{ref} = F_{net}\left(p_m \cdot \sigma_m + p_b \cdot \sigma_b\right) \qquad (9)$$

For a plate subjected to bending loads, F_{net} is determined assuming that the crack shape is rectangular, taking the displacement of the neutral axis into account. For a plate subjected to bending loads, JNC recommends that p_m=p_b=1.0.

Originally, the JNC method evaluates crack growth rate using J-integral range. However, in this benchmark, crack growth rate is related to the effective stress intensity factor range. The effective stress intensity factor range governing fatigue crack growth is determined by:

$$\Delta K_{eff} = \sqrt{\Delta J_{ep} \cdot E^*} \qquad (10)$$

where E^* is defined in eqn.(7).

4. *CEA Simplified Fatigue Crack Growth Evaluation Method – A16 document [6]*

In contrast to the JNC method, the A16 method uses the stress conditions obtained elastically in the calculation of SIF. According to the following equations, the equivalent SIF range is determined :

$$\Delta K_{eq}^{\ 2} = \Delta K_I^{\ 2} + \Delta K_{II}^{\ 2} + \frac{1}{1-\nu}\Delta K_{III}^{\ 2} \qquad (11)$$

$$\Delta K_I = Max._{t,t'}\left[K_I(t) - K_I(t')\right]$$

$$\Delta K_{II} = Max._{t,t'}\left[K_{II}(t) - K_{II}(t')\right]$$

$$\Delta K_{III} = Max._{t,t'}\left[K_{III}(t) - K_{III}(t')\right]$$

where $K_i(t)$ and $K_i(t')$ are mode i SIFs calculated as a function of time.

For a bending plate containing a semi-elliptical notch, only the mode I SIF is considered. Similarly to the JNC method, the A16 uses the Newman and Raju solution[5] to calculate SIF as follows :

$$K_I = F \cdot \left[\sigma_m + H \cdot \sigma_b\right]\sqrt{\frac{\pi \cdot a}{Q}} \qquad (12)$$

where F, H and Q can be found in the reference [5].

In contrast to the JNC method, the A16 uses the nominal membrane and bending stress, calculated elastically. The elastic J-integral range ΔJ_{el} is derived from ΔK_{eq}, such as :

$$\Delta J_{el} = \frac{\Delta K_{eq}^{\ 2}}{E^*} \qquad (13)$$

where E^* is defined in eqn.(7).

The elastoplastic J-integral range ΔJ_{sA16} is given by :

$$\Delta J_{sA16} = \Delta J_{el} \cdot k_{1A16} \cdot k_{2A16} \qquad (14)$$

where k_{1A16} and k_{2A16} are plastic correction factors. The first factor k_{1A16} is determined as shown in **Fig.3(a)** and is expressed by :

$$k_{1A16} = \left(\frac{\Delta\sigma_{nor}}{\Delta\sigma_{no}} \right)^2 \qquad (15)$$

where $\Delta\sigma_{nor}$ is the equivalent nominal primary and secondary elastic stress range and $\Delta\sigma_{no}$ is the equivalent nominal stress range. The second factor k_{2A16} is expressed by :

$$k_{2A16} = \frac{1}{2} \cdot \frac{\Delta\sigma_{ref}^{\ 2}}{\Delta\sigma_{ref}^{\ 2} + (2R_{0.2})^2} + \frac{E \cdot \Delta\varepsilon_{ref}}{\Delta\sigma_{ref}} \qquad (16)$$

where $\Delta\sigma_{ref}$ and $\Delta\varepsilon_{ref}$ are the reference stress and strain range, respectively, which can be determined from a limit load analysis of the cracked component. The determination of $\Delta\sigma_{ref}$ and $\Delta\varepsilon_{ref}$ is illustrated in **Fig.3(b)**. $R_{0.2}$ is the 0.2% proof stress of the material obtained from monotonic tensile tests. The effective stress intensity factor range ΔK_{eff} is defined by :

$$\Delta K_{eff} = q_r \cdot \sqrt{E^* \cdot \Delta J_{sA16}} \qquad (17)$$

where q_r is a crack closure factor given by :

$$\begin{array}{lll} \text{for } R \geq 0 & : & q_r = 1 / (1 - 0.5R) \\ \text{for } R < 0 & : & q_r = (1 - 0.5R) / (1 - R) \end{array}$$

In **Fig.3(b)**, $\Delta\sigma_{def}^{P \cdot Q}$ for a plate subjected to bending loads is given by :

$$\Delta\sigma_{def} = \left| \frac{\Delta\sigma_b}{3} \right| + \sqrt{\left(\frac{\Delta\sigma_b}{3} \right)^2 + \Delta\sigma_m^{\ 2}} \qquad (18)$$

$$\Delta\sigma_m = \frac{\Delta F}{2w \cdot t - (\pi \cdot a \cdot c/2)}$$

$$\Delta\sigma_b = \frac{6\Delta F \cdot L}{2w \cdot t^2}$$

where $\Delta\sigma_m$ and $\Delta\sigma_b$ are the membrane and bending stress range, respectively, ΔF is the applied load range, a and 2c are the crack depth and length, respectively.

5. Discussion

The calculated crack shape according to the JNC and A16 procedures at R=0.1 are compared with the experimental data in **Fig.4** and **Fig.5**. On these figures, fully elastic (E) and elastoplastic (EP) calculations are shown. At this load ratio, it is found that both methods provides predictions in good agreement with each other. At room temperature, a better correlation between the predictions and the experimental data is obtained with the elastic calculations than with the elastoplastic calculations as shown in **Fig.4**. At 650°C, the elastoplastic calculations give very good predictions of the crack shape throughout the duration of the experiments as shown in **Fig.5**.

The results obtained at R= –1.0 are shown in **Fig.6**. It is found that the A16 procedure leads to faster crack growth than the JNC procedure. This is essentially due to different values of the crack closure factor. **Figure 7** shows the relationship between load ratio and the crack closure factors. A remarkable difference can be seen between q_{A16} and q_{JNC}. At R=–1.0, q_{A16}=0.75 and q_{JNC}=0.5. When using the q factor proposed by JNC with the A16 procedure, a better correlation between the results is obtained. The discrepancies that

remain are due to :

*(1) The reference stress that accounts for the net section decrease on both σ_m and σ_b is used in the JNC procedure. **Figure 8** shows the variation of the reference stress with crack growth at 650°C and R=0.1. In the later stage of crack growth, the effect of the net section decrease cannot be ignored.*

(2) The JNC procedure uses the maximum stress in a load cycle whilst in the A16 procedure, the stress range is considered.

(3) For the calculation of SIF, JNC uses elastic membrane and bending stresses corrected to account for plasticity. In contrast, the A16 document recommends to use the elastic nominal stresses.

(4) In the plastic correction procedures, the following differences can be pointed out :

- *The plastic zone size correction in f_{cp} and $k_{2\,A16}$ are slightly different, depending upon the reference of the document used by JNC and the A16.*
- *In the definition of the yield stress, JNC uses the 0.2% proof stress on the cyclic stress-strain curve. In contrast, the A16 uses the 0.2% proof stress on the monotonic tensile curve.*

6. Conclusions

Benchmark problems consisting in predicting fatigue crack growth in 316L(N) cracked plates subjected to cyclic bending loads were solved. The predictions according to the JNC and A16 methods were compared with each other. At R=0.1, both procedures well predict the crack growth behavior observed experimentally. At R=−1.0, discrepancies are observed. Experimental data are necessary to better understand the crack closure behavior for this type of component.

Acknowledgement

The contribution of Mr.F.Curtit from Ecole des Mines of Paris is acknowledged. The JNC author also appreciates Mr.I.Furuhashi for his contribution in the development of the JNC method.

References

[1] Chapuliot S. et al., "Fatigue Growth of Semi-elliptical Cracks in Plates Subjected to Bending", Proceedings of PVP96 Vol.323, Fatigue and fracture Vol.1 (Jul./1996).

[2] Poussard C. et al. "High temperature leak before break experimental studies of austenitic stainless steel centre cracked plate", SMiRT 14, G13/5 (17-22/Aug./1997).

[3] C.Poussard et al. "Creep-fatigue Crack Growth in Austenitic Stainless Steel Centre Cracked Plates at 650 °C - Part I : Experimental Study and Interpretation", International 'HIDA' Conference, S3-22 (15-17 / Apr. / 1998).

[4] RCC-MR, 1993, Design and Construction Rules for Mechanical Components of FBR Nuclear Islands, 3rd edition, AFCEN, FRANCE.

[5] Newman J. and Raju I., "Analyses of Surface Cracks in Finite Plate under Tension or Bending Loads", NASA Technical Paper 1578 (1979).

[6] Drubay B. et al., "A16 : Guide for Defect Assessment and Leak Before Break Analysis", RAPPORT DMT 96.096 (Third draft - 31/Dec./1995).

Table 1 Description of the benchmark problems

	Test conditions				Geometry of plate		Length of	Initial notch		Exp.
	Temp. T (^{o}C)	Load ratio R -	Min.Load F_{min} (kN)	Max.Load F_{max} (kN)	Thickness t (mm)	Width $2w$ (mm)	Bending arm L (mm)	Depth a (mm)	Length $2c$ (mm)	data available
Benchmark-1	R.T.	0.1	3.12	31.2	20.0	350	350	6.0	81.0	1
Benchmark-2	650	0.1	1.9	19.0	24.5	350	370	2.5	85.0	2
Benchmark-3	650	-1.0	-14.0	14.0	24.5	350	350	2.5	85.0	0

Table 2 Material propeties

	Temperature T (^{o}C)	Mechanical properties			Fatigue crack growth Characteristics	
		Young's modulus E (MPa)	Poisson's ratio ν -	0.2% proof stress σ_y (MPa)	C_f -	m_f -
Benchmark-1	R.T.	195500	0.30	266	1.2×10^{-8}	2.84
Benchmark-2	650	140600	0.30	125	3.2×10^{-7}	2.46
Benchmark-3	650	141100	0.30	125	6.2×10^{-8}	3.28

Table 3 Cyclic stress-strain curve of 316L(N) at R.T.

$\Delta\sigma$ (MPa)	0	340	514	568	624	688	744	866	972	1060
$\Delta\varepsilon$ (mm/mm)	0.0000	0.0017	0.0040	0.0060	0.0080	0.0120	0.0160	0.0240	0.0300	0.0360

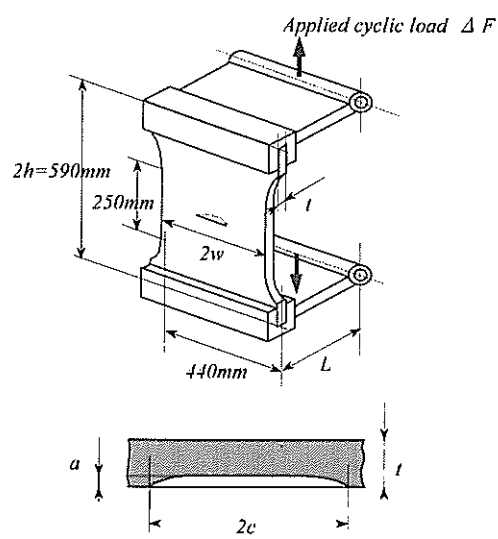

Fig. 1 Shape and dimensions of the specimen

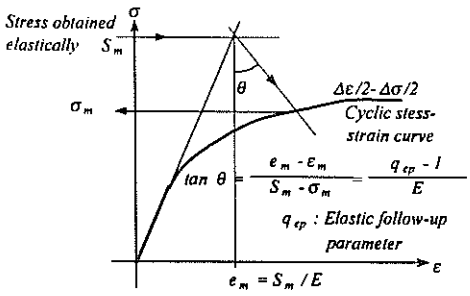

(a) Estimation of σ_m

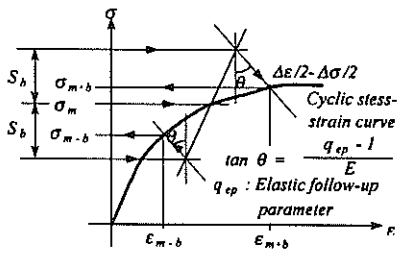

(b) Estimation of elastoplastic stress distribution

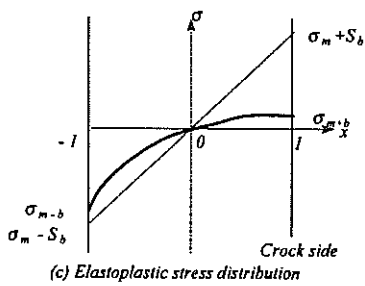

(c) Elastoplastic stress distribution

Fig.2 Determination of σ_m and σ_b according to the JNC method

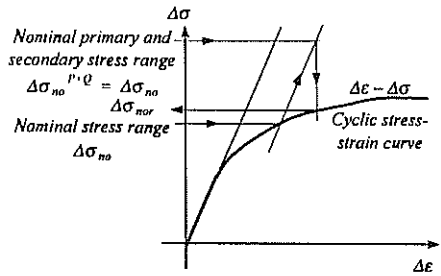

(a) Nominal stresses

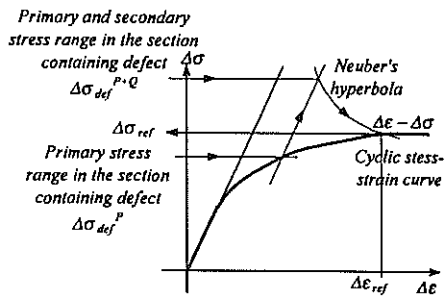

(b) Stresses in the ligament

Fig.3 Determination of $\Delta\sigma_{nor}$, $\Delta\sigma_{no}$ and $\Delta\sigma_{ref}$ according to the A16 method

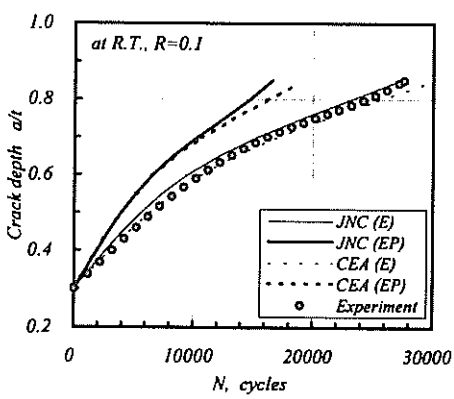

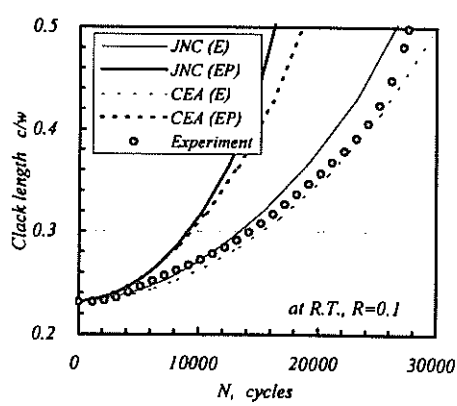

Fig.4 Comparison between calculated crack shapes and experimental data (at R.T., R=0.1)

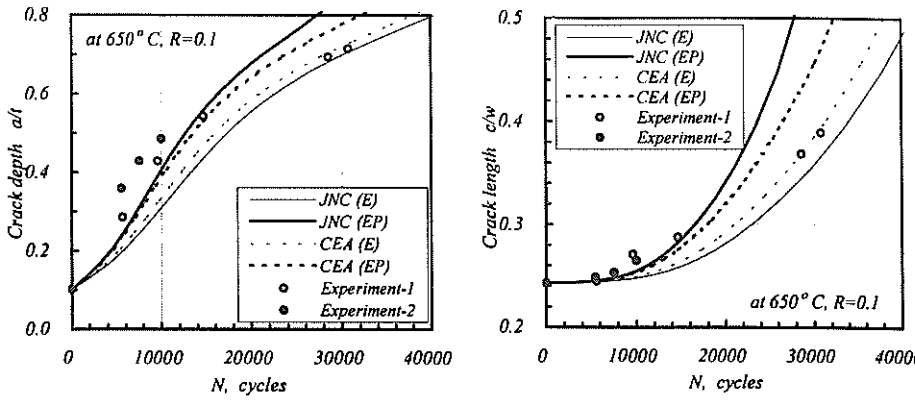

Fig.5 Comparison between calculated crack shapes and experimental data (at 650° C, R=0.1)

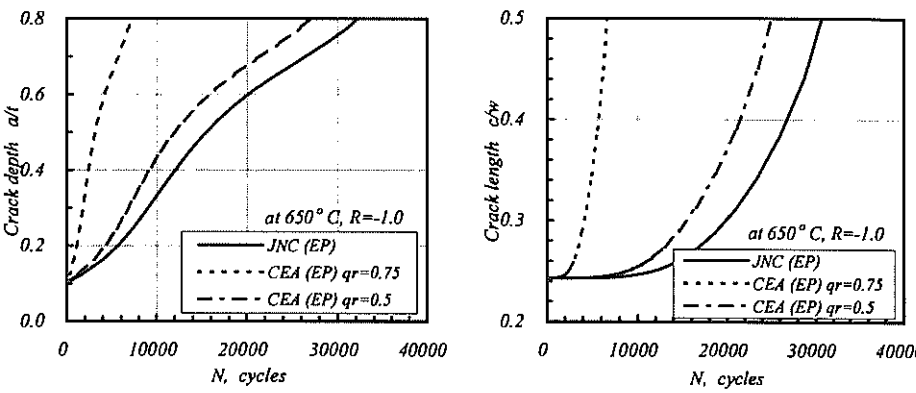

Fig.6 Comparison between calculated crack shapes (at 650° C, R=-1.0)

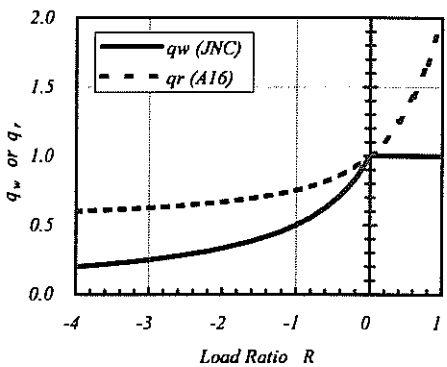

Fig.7 Crack closure factors

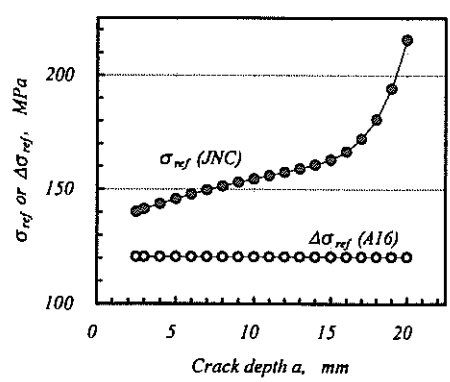

Fig.8 Variation of the reference stress with crack growth